

D.S. Krylov, O.I. Kholod

## Active rectifier with a fixed modulation frequency and a vector control system in the mode of bidirectional energy flow

**Goal.** Creation of a vector control system with improved characteristics for an active rectifier-voltage source operating in the bidirectional energy flow mode with a fixed modulation frequency. **Methodology.** The physical prerequisites for the active rectifier - voltage source operation in the system of a medium-power frequency electric drive are considered. A vector control system with a fixed modulation frequency is constructed, the principles of forming the signals acting in it and the influence on its operation of the converter power circuit parameters and the power consumed by it are considered. Mathematical modeling of the converter with the developed control system in MATLAB/Simulink made it possible to verify the correctness of the operation of the power circuit and the control system. **Results.** A new structure of a vector control system operating with a fixed modulation frequency is proposed, and the performance characteristics of the circuit in a wide range of changes in the magnitude and sign of the output power are obtained. The advantages of the new control system over the existing ones are shown. **Originality.** The physical prerequisites for the functioning of the power scheme and the vector control system of the ARVS proposed by the authors with a fixed frequency of modulation, the principles of forming the signals operating within it are considered in detail. **Practical significance.** New structure of the vector control system operating with a fixed modulation frequency is proposed and the advantages of the new control system over the existing ones are shown. References 17, tables 1, figures 9.

**Key words:** active rectifier, fixed modulation frequency, vector control system, bidirectional energy flow, vector diagram, coordinate transformation, pulse width modulation.

*В статті розглянуто роботу активного випрямляча-джерела напруги, що працює з фіксованою частотою модуляції в режимі двонаправленого потоку енергії, запропоновано нову структуру векторної системи управління, та отримано характеристики роботи схеми в широкому діапазоні зміни величини та знаку вихідної потужності. Розглянуті фізичні передумови функціонування силової схеми АВДН, запропонованої авторами векторної системи управління та принципи формування діючих усередині неї сигналів в складі частотного перетворювача середньої потужності. Показано переваги нової системи управління над існуючими та отримано залежності, що демонструють коректність застосування запропонованих у статті технічних рішень. Результати математичного моделювання показали, що АВДН, який працює з фіксованою частотою модуляції та запропонованою системою управління, дозволяє підтримувати задане значення вихідної напруги та близький до синусоїди струм мережі живлення при нульовому споживанні реактивної потужності в усталеному режимі в широкому діапазоні зміни параметрів схеми та величини і знаку потужності навантаження. Бібл. 17, табл. 1, рис. 9.*

**Ключові слова:** активний випрямляч, фіксована частота модуляції, векторна система управління, двонаправлений потік енергії, векторна діаграма, перетворення координат, широтно-імпульсна модуляція.

**Introduction.** The frequency converter is an integral part of industrial installations that use an induction motor (IM) as part of their composition. By changing the effective value and frequency of the three-phase alternating voltage supplied to the stator windings, it allows to implement various strategies for controlling the speed and torque on the shaft of this type of electric machine. In the range of small and medium powers when powered from an industrial network of 380-400 V, the converter structure based on an autonomous voltage inverter (AVI) has become the most widespread. It contains two main components: a converter of three-phase alternating voltage into direct one – a rectifier and an inverter powered by its output voltage, most often made according to a three-phase bridge circuit on alternating current switches.

The use of various modulation algorithms allows such an inverter to generate a voltage with the necessary parameters on the load and to adjust them within wide limits. Among the possible options, pulse-width, frequency-pulse, time-pulse and vector-pulse modulation [1-3] can be distinguished, each of which has its own advantages and disadvantages.

For AVIs operating in the range of small and medium powers, pulse width modulation (PWM) has become the most common. Having a relative simplicity of implementation, it provides a fixed switching frequency of valves switching in the circuit, which significantly simplifies their thermal calculation, and also facilitates the calculation of filters at the output of the circuit [4, 5].

A three-phase bridge diode circuit can act as a rectifier in the considered structure. Simple and reliable, here it has a number of significant disadvantages: it distorts the shape of the power network current; does not form a sufficient level of voltage at the input of the AVI when it operates in the sinusoidal PWM mode; does not ensure the return of energy from the load to the power network [1, 6].

Modern requirements for the quality of energy consumed from the industrial network force us to consider other topologies of rectifiers that are devoid of the mentioned disadvantages. Among them, we can single out a diode rectifier with various circuits of power factor correction modules, a rectifier according to the Vienna circuit and an active rectifier-voltage source (ARVS) circuit made, similarly to AVI, according to a three-phase bridge circuit on alternating current switches [1, 7, 8].

It is worth noting that only the ARVS circuit allows to simultaneously eliminate all the shortcomings inherent in the diode rectifier in the structure of the frequency converter based on AVI. Its effectiveness will also depend on the modulation algorithm used and the structure of the control system that implements it. For the same power circuits of ARVS and AVI in a single converter, it is advisable to use the same modulation algorithms and structures of control systems built on similar principles.

In modern practice, the strategies for controlling speed and torque on the shaft of an induction motor, built

© D.S. Krylov, O.I. Kholod

on the principles of presenting stator currents and voltages in the form of generalized vectors in different coordinate systems, have shown the greatest efficiency. They are implemented by the so-called «vector» control systems of autonomous inverters [7, 9].

ARVS control systems can be built according to a similar principle [10-13].

**The goal of the work** is to create a vector control system with improved characteristics for an active rectifier-voltage source operating in the mode of bidirectional energy flow with a fixed modulation frequency.

**Power circuit of the converter.** Figure 1 shows a generalized functional diagram of a frequency converter with an ARVS in the input circuit. It consists of the following components: *AC* – three-phase network of sinusoidal variable voltage  $u_s$ ; phase inductance  $L$ , including additional input reactors; active rectifier *AR*, made according to a three-phase bridge circuit on alternating current switches; direct current section of the converter *DC* with capacitive energy storage  $C$ , which smoothes out voltage ripples and creates an operating mode for the load that is close in characteristics to the voltage source; load *Load*, which is an AVI with PWM, which powers an induction motor.

The physical processes in each phase of the ARVS input circuit are similar to the other two with a shift of 120 electrical degrees. Consider them on the example of the equivalent circuit shown in Fig. 2.

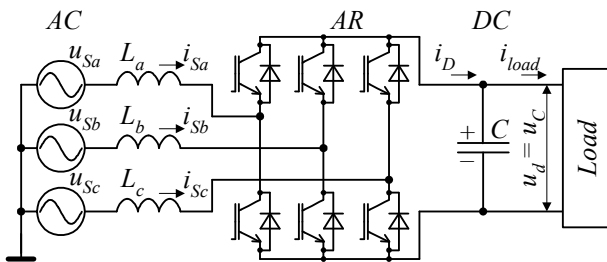


Fig. 1. Functional diagram of the converter with ARVS

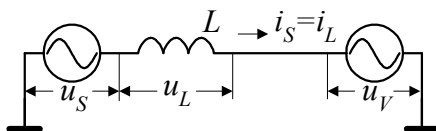


Fig. 2. Equivalent circuit of the ARVS input circuit phase

It contains: the source of sinusoidal alternating phase voltage with instantaneous value  $u_s$ ; the instantaneous phase voltage at the input of the ARVS  $u_V$ , which is formed during the operation of the semiconductor switch of the circuit in PWM mode, by periodically connecting to the phase of the power supply network the voltage on the capacitor of the DC link  $u_c = u_d$  with different polarity. As a result, during the modulation period, the sign of the voltage drop  $u_L$  on the input inductance of the phase  $L$  and the dynamics of the current  $i_L$  flowing through it change. This allows to form the required shape and phase of the current of the power source.

According to Kirchhoff law, at any moment in time, the instantaneous circuit voltages (Fig. 2) will be related to each other by the expression

$$u_S = u_L + u_V. \quad (1)$$

The generalized vector diagram for the input circuit of the ARVS phase while maintaining a unit power factor is shown in Fig. 3, *a* for the energy consumption mode, and in Fig. 3, *b* – for the energy recovery mode from the load to the power supply network.

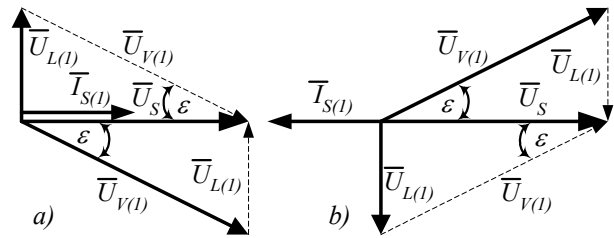


Fig. 3. Generalized vector diagram of the ARVS input circuit at a unit power factor for: *a* – energy consumption by the load; *b* – energy recovery from the load to the power supply network

The presence of the inductance  $L$  gives the ARVS input circuit the properties of a current source, which allows the circuit to operate in the boost PWM mode and maintain the voltage on the capacitor  $u_c = u_d$  of the DC link above the mains voltage.

By controlling the amplitude and phase shift angle  $\epsilon$  of the voltage  $u_V$ , it is possible to control the amplitude and phase of the source current  $i_S$  by varying the voltage drop across the input inductance  $u_L$ . Here, the average value and sign of the current at the output of the ARVS will be proportional to the active power at the input of the circuit. The reactive power can be controlled independently by shifting the current of the fundamental harmonic  $i_S$  with respect to the voltage  $u_s$ .

**Control system.** If we talk about the strategy of building the ARVS control system, it is often based on the dual identity of its power circuits with the AVI circuit as part of the general frequency converter. Indeed, the power circuits of both converters are exactly the same. Both have a common DC link that has the properties of a voltage source and their own circuits of three-phase alternating voltage, which, due to the serial connection of inductances in their phases, have the properties of current sources. Both provide a bidirectional flow of energy, because they operate as a step-down pulse width converter when transferring it from a DC link to an AC link and as a step-up one when transferring it from an AC link to a DC link. Therefore, it is possible to use the concepts of building AVI control systems to regulate an induction electric motor during the creation of ARVS control systems.

The main concepts of induction motor control are *Direct Torque Control* (DTC) and *Field Oriented Control* (FOC) [10, 11, 14]. They are matched with the strategy of *Direct Power Control* (DPC) and *Voltage Oriented Control* (VOC), which are used in ARVS [10, 11, 14, 15]. Each of them has many implementation options that have their own advantages and disadvantages.

Note that only ARVS vector control systems built on the basis of the *VOC* concept operate with a fixed modulation frequency. They are based on the principle of presenting generalized network current and voltage vectors in rotating (for example, *d-q*) coordinates, in which the regulated values are constant signals, which allows for the elimination of static control errors. Here, the structure of separate control of the «active»  $i_d$  and

«reactive»  $i_q$  components of the network current is used using its own, usually proportional-integral (PI) regulators for each of the channels. By adjusting the  $d$ -component of the current, it is possible to control the flow of energy between the source and the load, as well as to maintain the required voltage level on the capacitor of the DC link. The regulator of the  $q$ -component relies only on the function of maintaining a zero or other specified shift angle between the current and the voltage of the power supply network. This fully corresponds to the principle of operation of ARVS power circuits described above.

Vector control systems of ARVS using separate control structures are widely presented in [9-14]. Their essential drawback is the need for a direct and inverse transformation of the coordinates of the generalized current and voltage vectors with the calculation of the trigonometric function of their angle of rotation. This complicates the physical implementation of such systems and places increased demands on its element base.

It is possible to simplify the ARVS vector control system, which operates with a fixed modulation frequency, if we use the above-described principle of the converter operation.

To form the required shape and phase shift of the network current  $i_S = i_L$ , it is necessary to control the voltage drop on the input inductance of the circuit  $u_L$  by adjusting the value and phase shift of the input voltage  $u_V$ . Its first harmonic, in turn, repeats the control voltage at the input of the *PWM* generator with some given transmission ratio.

Representing (1) in relative units, it is possible to obtain an expression for determining the *PWM* control voltage of the generator, which forms a given shape of the network current in the form

$$u_V^* = u_S^* - u_L^* = u_S^* - L \frac{di_L^*}{dt}, \quad (2)$$

where  $u_S^*$ ,  $u_V^*$ ,  $u_L^*$  and  $i_L^*$  are the relative phase voltages and current of the input circuit of the ARVS according to Fig. 2, for which the amplitudes of the nominal phase voltage and current of the power source are taken as the basic values, respectively.

Thus, with unchanged voltage of the power source, the task of the control system is reduced to the generation of the task signal of the phase current of the ARVS input circuit with the necessary parameters. It can be solved using the principle of separate regulation described above.

Figure 4 shows the structural diagram of the ARVS vector control system proposed by the authors, which operates with fixed modulation frequency.

Instantaneous values of three phase currents  $i_S^*$  and voltages  $u_S^*$  of the power supply network, reduced to relative units, are supplied to the *abc-dq* coordinate conversion unit. In it, using the Clark matrix, currents and voltages are converted from coordinates *abc* to coordinates  $\alpha\beta$  according to the expressions

$$\begin{bmatrix} i_\alpha^* \\ i_\beta^* \end{bmatrix} = \sqrt{\frac{2}{3}} \begin{bmatrix} 1 & -\frac{1}{2} & -\frac{1}{2} \\ 0 & \frac{\sqrt{3}}{2} & -\frac{\sqrt{3}}{2} \end{bmatrix} \cdot \begin{bmatrix} i_{Sa}^* \\ i_{Sb}^* \\ i_{Sc}^* \end{bmatrix}; \quad (3)$$

$$\begin{bmatrix} u_\alpha^* \\ u_\beta^* \end{bmatrix} = \sqrt{\frac{2}{3}} \begin{bmatrix} 1 & -\frac{1}{2} & -\frac{1}{2} \\ 0 & \frac{\sqrt{3}}{2} & -\frac{\sqrt{3}}{2} \end{bmatrix} \cdot \begin{bmatrix} u_{Sa}^* \\ u_{Sb}^* \\ u_{Sc}^* \end{bmatrix}. \quad (4)$$

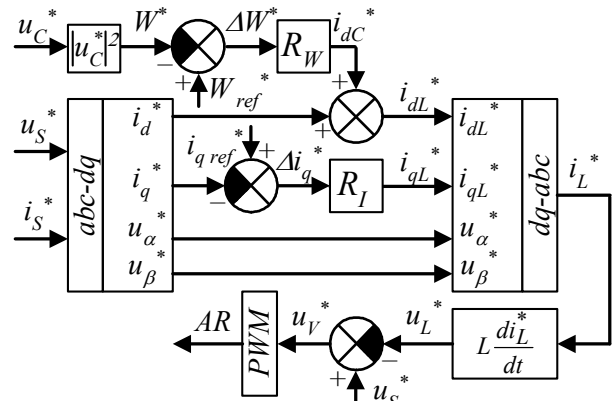


Fig. 4. Structural diagram of the ARVS control system

Then the relative instantaneous network currents are transformed from  $\alpha\beta$  coordinates to  $dq$  coordinates. If the Park matrix [16] is used directly for this, it will be necessary to calculate the trigonometric functions of the rotation angle of the generalized voltage vector of the power source. This increases the requirements for the hardware part of the control system. Therefore, it is advisable to obtain projections of the generalized network current vector on the  $dq$  axis through the coordinates of the generalized network voltage vector in the  $\alpha\beta$  system according to the expression [16]

$$\begin{bmatrix} i_d^* \\ i_q^* \end{bmatrix} = \frac{1}{\sqrt{u_\alpha^{*2} + u_\beta^{*2}}} \begin{bmatrix} u_\alpha^* & u_\beta^* \\ -u_\beta^* & u_\alpha^* \end{bmatrix} \cdot \begin{bmatrix} i_\alpha^* \\ i_\beta^* \end{bmatrix}. \quad (5)$$

In the mode of full reactive power compensation, the value of the  $q$ -projection of the generalized network current vector should tend to zero. This condition is valid both for the mode of energy consumption by the load and for the mode of energy recovery from the load to the power network. Therefore, the relative instantaneous value of the  $q$ -component of the network current  $i_q^*$  is compared with the task  $i_{q\text{ref}}^* = 0$ . The mismatch signal  $\Delta i_q^*$  is fed to the input of the PI current regulator  $R_I$ , which forms the  $q$ -component of the task current signal of the choke of the ARVS input circuit  $i_{qL}^*$ .

The flow of energy consumed or generated by the load depends on the operating modes of the load itself and in the structure under consideration (Fig. 1), controlled by the AVI control system. Therefore, there is no need to introduce any additional regulator of the  $d$ -component current of the ARVS network  $i_d^*$  into the shown in Fig. 4 structure of the control system. In this way, the proposed structure differs from most structures built on the basis of the concept of *VOC* [9-15].

The regulator is necessary to maintain the constant value of the voltage on the capacitor of the DC link at the level higher than the amplitude of the line voltage of the source. It needs to form the component  $i_{dC}^*$ , which complements  $i_d^*$  depending on the value and direction of the energy transmitted in the converter. At the same time,



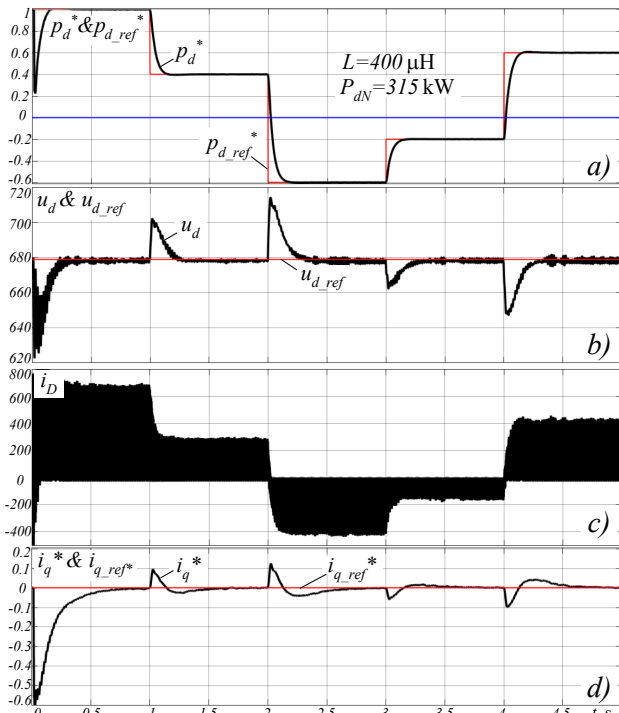


Fig. 7. Machine diagrams of the operation of the ARVS circuit

Figure 7,a shows the current value of the relative instantaneous power of the load and the step-changing task signal with different polarities. It can be seen that the power regulator performs the task correctly.

Figure 7,b shows the task signal and the current instantaneous value of the voltage of the DC link. It can be seen that in the steady state, the voltage regulator maintains its level exactly in accordance with the task, and the deviation of the instantaneous voltage level in transient modes does not exceed 8 % of the set value. The voltage task on the capacitor is selected at a level that exceeds the nominal amplitude of the line voltage of the power source by 20 %, which at given line voltage of 400 V is 678.8 V.

Figure 7,c shows the instantaneous value of the current at the ARVS output. It can be seen that it is modulated by high frequency and changes its polarity when the sign of the load power changes.

Figure 7,d shows the relative instantaneous value of the q-component of the ARVS network current  $i_q^*$ . It can be seen that in the steady state, its value tends to zero, that is, the level set by the regulator, which indicates the absence of consumption or generation of reactive power by the circuit, regardless of the value and sign of the power in the load.

Figures 8,a,b show the instantaneous values of the current and voltage of phase A in the mode of consumption (Fig. 8,a) and recovery (Fig. 8,b) of the load power at the level  $\pm 180$  kW.

It can be seen that the phase current has a sinusoidal shape and is in phase or in antiphase with the source voltage in the steady state.

Machine diagrams shown in Fig. 7, 8, testify to the correct operation of the ARVS with fixed modulation frequency and the proposed control system in all permissible operating modes.

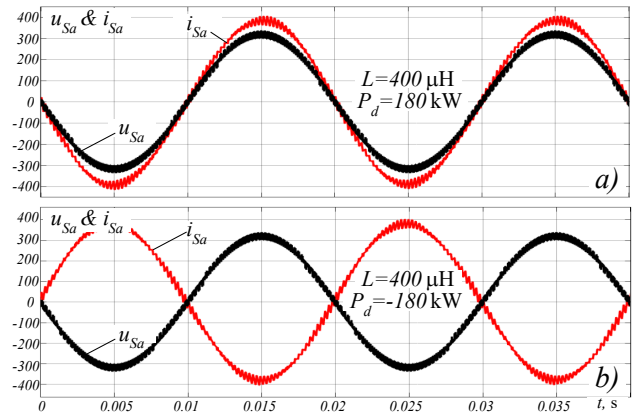


Fig. 8. Machine diagrams of current and voltage of phase A of ARVS

With the help of the model (Fig. 5), the dependencies of the total harmonic distortion coefficient of the current ( $THD_I$ ) and voltage ( $THD_U$ ) of the phase at the input of the converter on the relative value of the power of the circuit, which is consumed or generated by the load, are obtained. The studies were carried out for two values of the inductance of the ARVS input reactor. The obtained results are shown in the Table 1.

Table 1

Experimental research data

| $P_d^*$ | $THD_I, \%$         |                     | $THD_U, \%$         |                     |
|---------|---------------------|---------------------|---------------------|---------------------|
|         | $L=200 \mu\text{H}$ | $L=400 \mu\text{H}$ | $L=200 \mu\text{H}$ | $L=400 \mu\text{H}$ |
| 1       | 4.2                 | 2.46                | 10.24               | 5.46                |
| 0.8     | 5.3                 | 3.1                 | 10.25               | 5.47                |
| 0.6     | 7.1                 | 4.1                 | 10.25               | 5.48                |
| 0.4     | 10.1                | 5.7                 | 10.23               | 5.49                |
| 0.2     | 20.5                | 11.2                | 10.22               | 5.5                 |
| 0       | –                   | –                   | 10.2                | 5.48                |
| -0.2    | 21.8                | 12.2                | 10.16               | 5.46                |
| -0.4    | 11.0                | 5.9                 | 10.14               | 5.44                |
| -0.6    | 7.2                 | 3.9                 | 10.12               | 5.42                |
| -0.8    | 5.7                 | 3.1                 | 10.11               | 5.39                |
| -1      | 4.5                 | 2.5                 | 10.07               | 5.35                |

According to the Table 1 graphical dependencies of  $THD_I$  and  $THD_U$  at the connection point of the converter on the relative value of the power of the circuit, which is consumed or generated by the load, which are shown in Fig. 9 are built. Also in Fig. 9, the dashed line shows the acceptable values of  $THD_I$  and  $THD_U$ , which are 5 % and 8 %, respectively, according to the norms [17].

From the obtained graphical dependencies (Fig. 9), it can be concluded that with the input inductance  $L$  taken at the level of 400  $\mu\text{H}$ , the values of  $THD_I$  and  $THD_U$  correspond to the established standards in the entire range of changes in the power of the circuit, which is consumed or generated by the load. When reducing the value of the input inductance, to obtain the required  $THD_I$  and  $THD_U$  indicators it is necessary to install an additional input filter.



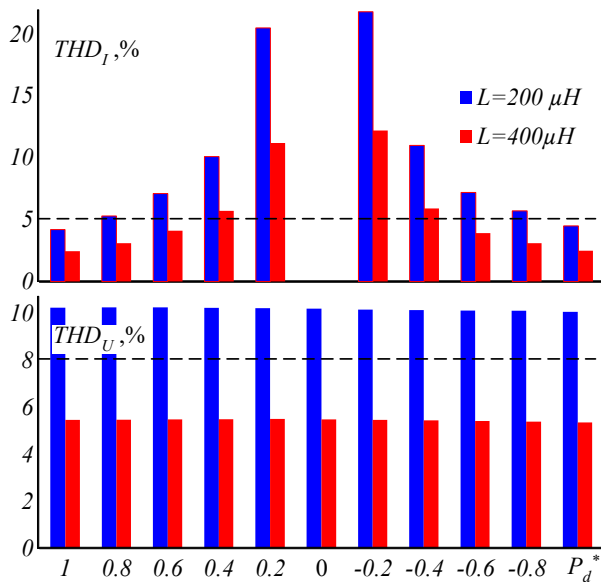


Fig. 9. Graphic dependencies of  $THD_I$  and  $THD_U$

### Conclusions.

1. The article proposes a new vector control system for an active rectifier-voltage source operating in the mode of bidirectional energy flow with fixed modulation frequency. It ensures stable and correct operation of the converter and has significant advantages compared to known vector control systems, namely: it reduces the number of regulators in the system to two; does not require calculation of  $d-q$  voltage components; does not require the calculation of trigonometric functions when transforming coordinates.

2. The article examines in detail the physical prerequisites for the operation of the power circuit and the ARVS vector control system with fixed modulation frequency proposed by the authors, as well as the principles of forming signals operating within it.

3. Mathematical modelling of the converter with the proposed vector control system in the MATLAB/Simulink software environment showed that the ARVS circuit allows maintaining a close to sinusoidal current of the power supply network and a set value of the output voltage with zero reactive power consumption in the steady state for a wide range of changes in the value and sign of the load power. The obtained machine diagrams allow to verify the correctness of the operation of the power circuit and the control system, which ensures minimal deviations from the specified parameters during transient processes.

**Conflict of interest.** The authors of the article declare that there is no conflict of interest.

### REFERENCES

1. Kolar J.W., Friedli T. The Essence of Three-Phase PFC Rectifier Systems – Part I. *IEEE Transactions on Power Electronics*, 2013, vol. 28, no. 1, pp. 176-198. doi: <https://doi.org/10.1109/TPEL.2012.2197867>.
2. Nandhini E., Sivaprakasam A. A Review of Various Control Strategies Based on Space Vector Pulse Width Modulation for the Voltage Source Inverter. *IETE Journal of Research*, 2022, vol. 68, no. 5, pp. 3187-3201. doi: <https://doi.org/10.1080/03772063.2020.1754935>.
3. Jalnekar R.M., Jog K.S. Pulse-Width-Modulation Techniques: A Review. *IETE Journal of Research*, 2000, vol. 46, no. 3, pp. 175-183. doi: <https://doi.org/10.1080/03772063.2000.11416153>.

### How to cite this article:

Krylov D.S., Kholod O.I. Active rectifier with a fixed modulation frequency and a vector control system in the mode of bidirectional energy flow. *Electrical Engineering & Electromechanics*, 2023, no. 6, pp. 48-53. doi: <https://doi.org/10.20998/2074-272X.2023.6.08>

4. Krylov D.S., Kholod O.I. Determination of the input filter parameters of the active rectifier with a fixed modulation frequency. *Electrical Engineering & Electromechanics*, 2022, no. 4, pp. 21-26. doi: <https://doi.org/10.20998/2074-272X.2022.4.03>.
5. Kim H., Sul S.-K. A novel filter design for output LC filters of PWM inverters (2011) *Journal of Power Electronics*, 11 (1), pp. 74-81. doi: 10.6113/JPE.2011.11.1.074.
6. Yazdavar A.H., Azzouz M.A., El-Saadany E.F. Harmonic Analysis of Three-Phase Diode Bridge Rectifiers Under Unbalanced and Distorted Supply. *IEEE Transactions on Power Delivery*, 2020, vol. 35, no. 2, pp. 904-918. doi: <https://doi.org/10.1109/TPWRD.2019.2930557>.
7. Premkumar K., Kandasamy P., Vishnu Priya M., Thamizhselvan T., Ron Carter S.B. Three-phase rectifier control techniques: A comprehensive literature survey. *International Journal of Scientific and Technology Research*, 2020, vol. 9, no. 1, pp. 3183-3188.
8. Dwivedi A., Tiwari A.N. Analysis of three-phase PWM rectifiers using hysteresis current control techniques: a survey. *International Journal of Power Electronics*, 2017, vol. 8, no. 4, pp. 349-377. doi: <https://doi.org/10.1504/IJPELEC.2017.085201>.
9. Krylov D., Kholod O., Radohuz S. Active rectifier with different control system types. *2020 IEEE 4th International Conference on Intelligent Energy and Power Systems (IEPS)*, 2020, pp. 273-278. doi: <https://doi.org/10.1109/IEPS51250.2020.9263226>.
10. Soeiro T.B., Friedli T., Kolar J.W. Design and Implementation of a Three-Phase Buck-Type Third Harmonic Current Injection PFC Rectifier SR. *IEEE Transactions on Power Electronics*, 2013, vol. 28, no. 4, pp. 1608-1621. doi: <https://doi.org/10.1109/TPEL.2012.2209680>.
11. Wang Y. *Analysis of three-phase rectifier via three different control methods and switch power loss comparison*. Mankato, Minnesota State University, 2021. 93 p.
12. Krylov D.S., Kholod O.I. The efficiency of the active controlled rectifier operation in the mains voltage distortion mode. *Electrical Engineering & Electromechanics*, 2021, no. 2, pp. 30-35. doi: <https://doi.org/10.20998/2074-272X.2021.2.05>.
13. Zhang C., Yu S., Ge X. A Stationary-Frame Current Vector Control Strategy for Single-Phase PWM Rectifier. *IEEE Transactions on Vehicular Technology*, 2019, vol. 68, no. 3, pp. 2640-2651. doi: <https://doi.org/10.1109/TVT.2019.2895290>.
14. Liu C., Luo Y. Overview of advanced control strategies for electric machines. *Chinese Journal of Electrical Engineering*, 2017, vol. 3, no. 2, pp. 53-61. doi: <https://doi.org/10.23919/CJEE.2017.8048412>.
15. Kumar R., Gupta R.A., Bhangale S.V. Vector control techniques for induction motor drive: a review. *International Journal of Automation and Control*, 2009, vol. 3, no. 4, pp. 284-306. doi: <https://doi.org/10.1504/IJAAC.2009.026778>.
16. Zhemerov G.G., Tugay D.V. *Coordinates transformation of general vectors of voltages and currents for a three-phase power supply system*. Kharkiv, O.M. Beketov NUUE Publ., 2020. 200 p.
17. *IEEE Std 519-2014. IEEE Recommended Practice and Requirements for Harmonic Control in Electric Power Systems*, 2014, pp. 1-29. doi: <https://doi.org/10.1109/IEEESTD.2014.6826459>.

Received 05.03.2023

Accepted 08.05.2023

Published 02.11.2023

D.S. Krylov<sup>1</sup>, PhD, Assistant Professor,

O.I. Kholod<sup>1</sup>, PhD, Senior Lecturer,

<sup>1</sup> National Technical University «Kharkiv Polytechnic Institute»,

2, Kyrpychova Str., Kharkiv, 61002, Ukraine,

e-mail: Denis.Krylov@khp.edu.ua (Corresponding Author);

Olha.Kholod@khp.edu.ua